International Journal of Engineering Science Invention
ISSN (Online): 2319 – 6734, ISSN (Print): 2319 – 6726
www.ijesi.org ||Volume 4 Issue 9|| September 2015 || PP.15-31

Simulation of Sediment Transport in the Canal Using the Hec-Ras (Hydrologic Engineering Centre - River Analysis System) In an Underground Canal in Southwest Kano Irrigation Scheme – Kenya

Ochiere H. O.[1], Prof. Onyando J. O.[2],Dr. Kamau D. N.[3]
[1]*(Engineering Department/ Egerton University, Kenya)*
[2]*(Engineering Department/ Egerton University, Kenya*
[3]*(Engineering Department/ Egerton University, Kenya)*

ABSTRACT*: The underground canal of Southwest Kano Irrigation scheme was designed to ensure that water is conveyed with minimal erosion and sedimentation but over time it has been silted up to the extent that its conveyance capacity has significantly dropped. This study is based on simulation of sediment transport within the underground canal in Southwest Kano Irrigation Scheme boundaries using Hydrologic Engineering Centre – River Analysis System (HEC-RAS) model. Ackers-White sediment transport equation, engraved in the model, was used to analyse sediment transport characteristics. The conceptual and physical parameters required in the HEC-RAS model were determined through calibration and direct measurement respectively. The model was calibrated based on the current operational conditions of the canal followed by simulation using the model to determine the sediment discharge and deposition rates at different levels of flow in the canal. The Ackers-White sediment transport equation predicted the sediment sizes which were deposited at specific sections of the canal at different flow rates. Higher flow rates resulted in minimal deposition. As a sediment management strategy, these sediment sizes could be screened off at the canal intake, to ensure that sediment passing through would be transported out to the canal outlet without deposition.*

KEYWORDS–*canal, flow, irrigation, sediment, simulation*

I. INTRODUCTION

All rivers and canals conveying water contain eroded sediments. Increase of soil erosion due to catchment degradation especially in developing countries has resulted into increased siltation problems in rivers as reported by Onyando et al. (2004). In this study it was found out that high sediment concentration in River Nyando is the main source of sediments in the Southwest Kano underground canal. Studies by McCully (1996) consider a river or canal, as a body of flowing sediments as much as one of flowing water. When flow in the canal is below the fall velocity of a given sediment size, the sediment would be deposited. As the sediments accumulate in the canal, the canal gradually loses its ability to transport water. Such canals lose water conveyance capacity due to sedimentation although the rate at which this happens varies widely. Sometimes the rate of sedimentation is higher than the rate at which revenue required for maintenance of the canal is submitted by the users. Canal sedimentation is the most serious technical problem facing irrigation systems (Depeweg and Mendez, 2006).

The proportion of sediments entering a diversion canal depends on the sediment load in the river source. Transport capacity is compared to the sediment load to determine whether detachment or deposition is occurring (Finkner et. al., 1989). Therefore deposition occurs when the sediment transport capacity of flow is less than the sediment load carried by the flow. The sediment deposited in the canal can be flushed out only if the transport capacity of the canal flow is increased. The sediments transported through flushing should be discharged at non-erosive velocity at the end of the canal.

The canal, which is the subject of this study, was constructed in Southwest Kano Irrigation Scheme, Kenya to convey water to rice fields through gravity flow. The water is abstracted from river Nyando through a 200 m long bypass canal before eventually getting channelled through an underground circular concrete-lined canal of diameter 1500 mm and 730 m long. The rest of the main water conveyance system consists of open trapezoidal canal with earth lining.

Southwest Kano intake canal was designed to convey irrigation water but due to continual siltation the capacity of the canal to convey water has been reduced by almost 50%. Maintenance of the open canal downstream is usually carried out by the bucket excavator but the underground section, being enclosed, is not accessible by the excavator. The underground section though accessible by humans, use of human labour for manual removal of the deposited sediment has not been feasible. It is therefore necessary to further understand the dynamics of sedimentation in the underground canal for the engineers to remedy the situation.

Design of most irrigation canals are based on flow regime principle. Ayibotele and Tuffour-Darko, (1979) found out that information on long-term sediment load, concentration and particle size distribution is important in the design of canals, and in the evaluation of quality of water. Therefore, simulation of sediment transport in the canal using the HEC-RAS (Hydrologic Engineering Centre – River Analysis System) would help isolate the sediment sizes contributing to the problemso that efforts could be concentrated on selective elimination of these sediments from the canal flow.A priori determination of sediments to be screened off would enable economic selection of screening materials and reduce the cost and frequency of desiltation as and when this occurs. Essentially it would enable the management of the canal to be more effective and achieve timely delivery of water to the rice fields.

Findings by Depeweg and Mendez, (2002) indicated that sediment transport in irrigation canals is always under changing flow conditions unlike the assumption of uniform and steady flow condition, which forms the basis of canal design. The author recommended the Ackers-White and Brownlie sediment transport equations for computation of sediment transport under equilibrium conditions and a numerical solution of Galappatti's depth integrated model for non-equilibrium state computations.

The characteristics of flow in canal systems are the driving force for sediment movement. River systems are characterized as open-channel flow systems, bounded by a free-surface. The shape of the free-surface must be established to allow the determination of hydraulic parameters needed for open-channel flow calculations. This water surface profile is often determined using an energy balance approach. Flow velocity, hydraulic radius, depth, roughness, sediment size, and other hydraulic parameters may then be used to predict the magnitude of sediment transport processes.

Attempts have been made to estimate bedload based on more easily measured parameters but these methods are not widely used since there is still much debate on their accuracy and reliability (Hudson, 1994). However a simple method, using suspended sediment concentration and texture of both suspended sediments and bed material, is shown in TABLE 1. Reliable bedload measurement is difficult to obtain because sampling devices affect the flow and bedload movement (Spillios, 1999). Measured bedload data appear to be random in nature and large fluctuations are experienced during relatively stable hydraulic and supply conditions (Xiaoqing, 2003)

Table 1: Maddock's classification for estimation of the bedload

Suspended sediment concentration (parts per million)	River bed material	Suspended elements texture	Bedload discharge expressed as % of suspended sediment discharge
less than 1000	sand	similar to the river bed	25-150
less than 1000	gravel, rocks, hard clay	low sand content	5-12
1000 - 7500	sand	similar to the river bed	10-35
1000 - 7500	gravel, rocks, hard clay	25% sand or less	5-12
more than 7500	sand	similar to the river bed	5-15
more than 7500	gravel, rocks, hard clay	25% sand or less	2-8

Source: Hudson, 1994.

Huang and Bountry (2009) suggested applicability of some of the most widely used methods to compute sediment transport based on sediment size as in TABLE 2.

Table 2: Commonly used sediment transport equations based on sediment size

Sediment size		
Sand	Gravel and sand	Gravel
Engelund and Hansen (1972)	Parker (1990)	Wilcock and Crowe (2003)
Ackers and White (1973)	Wilcock and Crowe (2003)	Parker (1990)
Yang (1973)	Wu (2004)	Meyer-Peter and Muller (1948)
Yang (1979)		Yang (1984)

According to studies by Depeweg and Mendez (2002), prediction of the sediment transport in irrigation canals within an error factor smaller than 2 is hardly possible. Even in the case of the most reliable method, only 61% of the values are predicted with a tolerance of error of ±100% compared to the measured values. The performance of sediment transport equations was reviewed by ASCE (1975) and study findings showed that the mean ratio of observed to predicted transport rate was between 0.5 and 2 for only 64% percent of the comparisons for the best method that was tested.

This study prefers Ackers-White for its flexibility, wide sediment class range and ability to compute total sediment load. Mean velocity is used as the representative parameter (US Army Corps of Engineers, 2002).

II. METHODOGY

2.1 Determination of Input Parameters into HEC – RAS model

The input parameters were both physical and conceptual as shown in TABLE3The value of each parameter was either measured directly or computed from hydrologic equations or was already engraved in the model.

Table 3: HEC-RAS input parameters and how they were determined

Physical variables/ Parameters		Means of determination
Symbol/unit	Description	
d (m)	Particle diameter	Determined from sieving sediment sample
D(m)	Water depth	Measured using tape measure and navigation rod
V(m/s)	Average flow velocity	Measured using the current meter
ν(m2/s),	Kinematic viscosity	Provided by HEC-RAS user manual as being computable from measured water temperature
g(m/s2)	Acceleration due to gravity	Constant provided in HEC-RAS user manual (10 m/s^2)
γ s(Kg/m2s2)	Sediment specific weight	Constant provided in HEC-RAS user manual (2.65 Kg/m2s2)
γ(Kg/m2s2)	Water specific weight	Provided by HEC-RAS user manual as being computable from measured water temperature
R(m)	Hydraulic radius	Model computation from measured depth and width of flow.
S(m/m)	Slope	Computed from elevation determined by the dumpy level.
T(^{o}C)	Water temperature	Measured using a thermometer
Conceptual Parameters		
Symbol (dimensionless)	Description	
m	Exponent	Calibration
n	Transition exponent	Calibration
C	Coefficient	Calibration
A	Critical mobility parameter	Calibration
α	Coefficient	Constant provided in HEC-RAS user manual (10) for turbulent flow

The sets of input data was determined for each section where the three manholes were positioned; that is between points A and B as shown in Fig. 1 and Fig. 2. Samples for determination of sediment size and percent composition were obtained from the bed of the channel reach and gradation done in the laboratory. During gradation the particles were screened using different sieves into various grain classes to determine the sediment size (diameter) distribution. Channel flow velocity, water depth, and water temperature were measured using current meter, tape measure and thermometer respectively. Bed slope was determined using dumpy level.

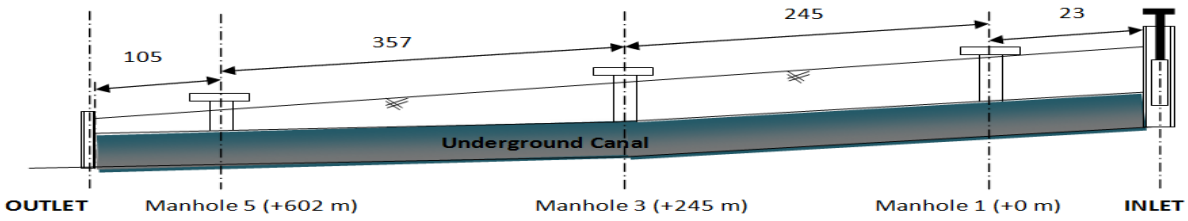

Figure 1: Sketch of Southwest Kano underground canal

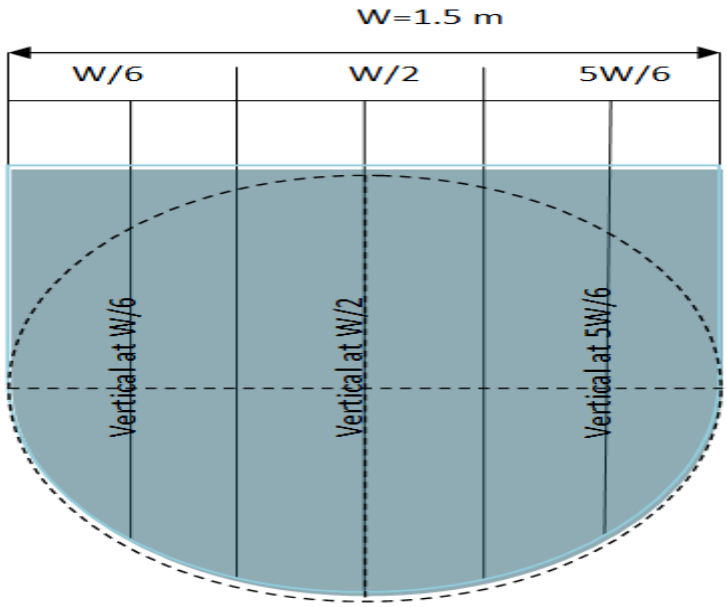

Figure1**:** Sketch of Southwest Kano underground canal cross section

The HEC-RAS model produced sets of results for each of the three canal cross sections, as in Fig. 2, between A and B with the outputs of sediment discharge for each input size of sediment material.

a. Calibration and Validation of HEC-RAS model

The HEC-RAS model was calibrated and validated in two steps. The first phase of calibration involved determination of Mannings n for steady flow which best fitted the observed surface. The value of n derived was used to calibrate conceptual parameters based on measured sediment transport values.

Sediment deposition rate was simulated by the HEC–RAS model given various input variables into Ackers and White sediment transport equation as defined by Ackers and White (1973). The output of the model was sediment discharge at different sections. Sediment deposition rate was obtained from the difference in the sediment discharge at the successive manholes. A temporal deposition limiter was applied by the HEC-RAS model using equations 16, 17, 18 for fall velocity to determine conditions for deposition and entrainment.

The HEC-RAS uses the input parameters outlined in TABLE 2 to calculate the sediment deposition rate as follows:

The value of grain diameter is used to calculate dimensionless grain diameter, dgr, as

$$d_{gr} = d\left[\frac{g}{\nu^2}\left(\frac{\gamma_s}{\gamma} - 1\right)\right]^{1/3} \quad (1)$$

whereν is viscosity and is dependent on temperature as shown in equation 8 below;

$$\nu = [1.14 - 0.31(T - 15) + 0.00068(T - 15)^2]10^{-6} \quad (2)$$

The transition exponent, n, the critical mobility factor, A, the coefficient, C, and the exponent, m, are determined by simulating the model based on sediment transport functions in TABLE 2.6.2. Water temperature, T, is measured using a thermometer in ^{o}C.

The particle mobility number, Fgr, is calculated as:

$$F_{gr} = U^{*n}\left[gd\left(\frac{\gamma_s}{\gamma} - 1\right)\right]^{-1/2}\left[\frac{v}{\sqrt{32}\log(\alpha D/d)}\right]^{1-n} \quad (3)$$

where U* is the shear velocity (m/s) given by:

$$U^* = \sqrt{gRS} \tag{4}$$

$$G_{gr} = 0 \qquad \text{if } A \geq Fgr \tag{5}$$

Sediment flux X, in parts per part by fluid weight was given by:

$$X = \frac{q_s}{q} = \frac{G_{gr}\, d}{D\left(\frac{U^*}{V}\right)^n} \tag{6}$$

Potential sediment discharge *G*, in kg/s

$$G = \frac{\gamma q X}{g} \tag{7}$$

where qs and q were sediment discharge and water discharge respectively.

This output is a product of the simulated model for various segments within the canal for each grain class. The total transport capacity, $T_{c,}$ for n number of grain classes with β_i percentage composition and α = 10 for turbulent flow.

The generalised dimensionless sediment transport rate is expressed as:

$$G_{gr} = \frac{q_s D}{qd}\left[\frac{U^*}{V}\right]^n = C\left[\left(\frac{F_{gr}}{A} - 1\right)\right]^m \qquad \text{if } A < Fgr \tag{8}$$

Otherwise,

of class i and Gi transport potential for class i is given by:

$$T_c = \sum_{i=1}^{n} \beta_i G_i \tag{9}$$

Transport potential is used to determine whether there is a deficit or surplus sediments in supply resulting into erosion or deposition respectively.

Deposition efficiency, Cd, is used to determine the boundary condition for erosion or deposition;

$$C_d = \frac{V_s(i)\Delta t}{D_e(i)} \tag{10}$$

where Vs(i) was the fall velocity of particle class i at time step Δt and De effective depth of water. For irregular section divided into subsections;

$$D_e = \frac{\sum_{i=1}^{n} D_{avg}\, a_i D_{avg}^{2/3}}{\sum_{i=1}^{n} a_i D_{avg}^{2/3}} \tag{11}$$

where ai is the area of subsection i , Davg the average depth of subsection i and n the number of subsections. Similarly effective width We is given by,

$$W_e = \frac{\sum_{i=1}^{n} a_i D_{avg}^{2/3}}{D_e^{5/3}} \tag{12}$$

Fall velocity Vs is computed using the Van Rijn equation as recommended by Depeweg and Mendez (2002). Thus,

$$V_s = \begin{cases} \dfrac{(s_s - 1)gd}{18\nu}; & 0.001 < d < 0.1mm \\ \dfrac{10\nu}{d}\left[\left(\dfrac{1 + 0.001(s_s - 1)gd^3}{\nu^2}\right)^{0.5} - 1\right]; & 0.1 < d < 1mm \\ 1.1[(s_s - 1)gd]^{0.5}; & d \geq 1\text{mm} \end{cases} \tag{13}$$

where S_s is the specific gravity of particles, v the kinematic viscosity, d particle diameter in millimeters and g the acceleration due to gravity.

Deposition occurred for Cd < 1 but for erosion or entrainment Cd > 1. At Cd = 1 neither deposition nor entrainment occurs.

The difference between sediment discharge at the inlet segment, q1, and the adjacent segment, q2, gives the sediment deposition rate. Therefore deposition rate D_r in Kg/s between sections 1 and 2 was given by:

$$D_r = G_1 - G_2 \tag{14}$$

$$D_r = \frac{\gamma q X}{g}(q_1 - q_2) \tag{15}$$

Sediment deposition rate was also computed from direct measurements of sediment load for calibration and validation and a graph of simulated versus measured values was plotted and analysed.

Calibration process involves adjustment of the model conceptual parameters within the margins of the uncertainties to obtain a model representation of sediment transport within the canal. The assessment can be done using regression analysis. If the simulated and the measured values do not closely relate, then the model would be calibrated by optimising the conceptual parameters A, C, m and n. The starting value of the parameter to be calibrated is based on documented guidelines and experience. This value is optimised until an optimisation parameter, P, is minimised. The equation for determination of P is given by;

$$P = \left(\sum_{i=1}^{t}(X_i - X_{ci})^2\right)^{1/2} \tag{16}$$

Where X is the measured value, Xc is the computed value for each data set i and t is the total number of data sets. The resulting parameter value is the calibrated value.

In addition, an average difference, Da, in the simulated and measured values is computed for N stations using,

$$D_a = \left(\sum_{i=1}^{t}\frac{(X_i - X_{ci})^2}{N}\right)^{1/2} \tag{17}$$

This represents the average error, over the study reach, where the computed value is above or below the measured value and provides an intuitive measure of the accuracy.

Validation process involves determining whether the values given by the model represent the acceptable range by comparing directly measured values and the model simulated output. The assessment can be done using regression analysis.

Validation process involves determining whether the values given by the model represent the acceptable range by comparing directly measured values and the model simulated output. The assessment can be done using regression analysis. The regression curve is used to estimate a variable Y by means of a variable X. The line can show whether there is a pronounced relationship between X and Y (Hoel, 1984). The closeness of the two variables is known as the correlation coefficient, r, given by

$$r = \frac{\sum_{i=1}^{n}(x_i - \bar{x})(y_i - \bar{y})}{(n-1)S_x S_y} \tag{18}$$

where i has values of 1, 2, 3,..., n; xi the ith sediment load direct measurement; yi the ith sediment load value from model output; n the sample size; Sx the variance of x; Sy the variance of y; $\bar{x}$ the mean value of x; and $\bar{y}$ the mean value of y.

The correlation coefficient, which ranges from −1 to 1, is an index denoting how closely related the observed and simulated data are. Value of r = 0, shows no linear relationship exists but for r = 1 or r = −1, a perfect positive or negative linear relationship exists respectively. The correlation coefficient, r2, measures the variance of the measured data. High values of r2 indicate comparatively less error and values higher than 0.5 are considered acceptable (Santhi et al., 2001). The fact that only the dispersion is quantified, it follows that if r2 is considered alone there could be errors of over-prediction or under-prediction even with values of r2 close to 1.0.

If r2 is used for model validation it is therefore advisable to take into account additional information which can cope with that problem. Such information is provided by the gradient, b , and the intercept, a, of the regression on which r2 is based. For a good agreement the intercept a should be close to zero which means that an observed value of zero would also result in a prediction near zero and the gradient b should be close to one. For a proper model assessment the gradient b should always be discussed together with r2. To do this in a more operational way the two parameters can be combined to provide a weighted version (wr2) of r2 (Krause, et al., 2005). Such a weighting can be performed by:

$$wr^2 = \begin{cases} |b| \cdot r^2 & \text{for } b \le 1 \\ |b|^{-1} \cdot r^2 & \text{for } b > 1 \end{cases} \tag{19}$$

By weighting r2 under-prediction or over-predictions are quantified together with the dynamics which results in a more comprehensive reflection of model results.

2.2 Simulation using HEC-RAS Model for 0.25, 0.50, 0.75, and full flow scenarios.

Simulation of HEC-RAS was done to analyse sediment transport within the canal before it got silted up. This involved use of calibrated values of conceptual parameters for the canal but with different value of Manning's n. The simulation was done for the selected scenarios for the purposes of plotting sediment rating curve. The value of Manning's n=0.017 was set for concrete channel assuming it was originally empty and had no initial deposited sediments. The depths derived from 0.25, 0.50, 0.75, and full flow scenarios were used to compute corresponding velocities using the Manning's equation:

$$V = \frac{1}{n} R^{2/3} S^{1/2} \tag{20}$$

where V is the velocity, n the Manning's roughness coefficient, R the hydraulic radius and S the bed slope. S was obtained from elevation measurements using the dumpy level and a navigation rod and n from the manuals. R was determined using geometrical relation for circles as in equation 21. Angle Ø (radians) was computed from the flow surface width, B, and flow depth, D, using the relation in equation 22 (see Fig. 3).

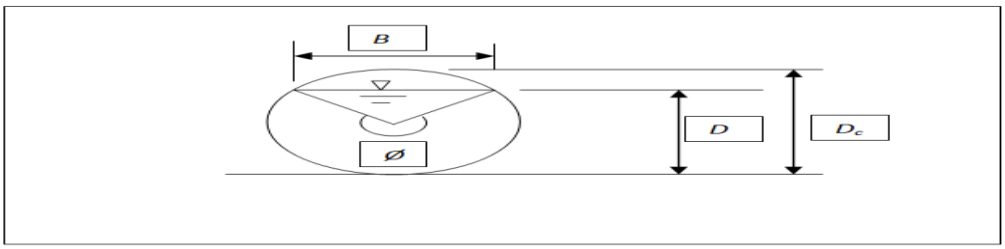

Figure 3: Canal cross section

$$R = \frac{1}{4}\left(1 - \frac{\sin \emptyset}{\emptyset}\right) D_c \tag{21}$$

where Ø was the angle subtended by the water surface from the centre of the canal and Dc the canal diameter.

$$\emptyset = 2 \sin^{-1}\left(\frac{B}{D}\right) \tag{22}$$

The HEC-RAS model was run with sets of input data for the specified scenarios to give respective outputs of sediment discharge and deposition rate at any time step, Δt. It was possible to tell which scenario had minimum deposition rate. It was also be possible to predict how much sediment would be deposited for a given duration.

III. RESULTS AND DISCUSSION

3.1 Calibration and Validation of HEC-RAS Model Based on Current Flow Conditions

The first phase of calibration involved Manning's roughness coefficient, n. The HEC-RAS model was run for steady flow equation using the concept of stream flow energy balance with a known water surface elevation downstream. Low flow values of profile PF2, profile PF3 and profile PF4 were used for calibration while higher flow values of profile PF1 and profile PF5 for validation since the calibrated Manning's roughness coefficient works best for high flow as observed by Parhi et al.,2012. The initial value of n was taken to be 0.013 for the whole canal as is recommended by Chow(1959) for concrete lined canals. The final calibrated values of Manning's n varied from one canal section to the next; with first manhole, Mh1, having n=0.032, third manhole Mh3, having n=0.011 and fifth manhole, Mh5, having n=0.011. These values were arrived using optimisation method as shown in equation 16 and 17. Calibration reduced the values of average difference, Da, hence reducing the error factor for profiles PF2, PF3 and PF4 by 43.5%, 46.5%, 27.8% respectively (see TABLE 4). The error factors encountered during calibration compared closely. Error factors for high flows were comparatively high. These high error values could have arisen from unaccounted for flow invariability due to intermittent open surface and pressurised flow segments between measurement stations.

The percentage weighted correlation coefficient, wR2 , ranged from 0.67 to 0.99 for both calibration and validation data as shown in TABLE 4, Fig. 4 and Fig. 5 with profile PF4 value of wR2 being 0.67. The other values of wR2 for calibration and validation were within the acceptable range of 0.5. The calibrated value of n = 0.032 at manhole Mh1 was above the recommended value for concrete lined canal, but suited a lined canal with gravel bottom and sides of dry rubble or riprap according to Chow (1959). This value was higher than expected meaning that there could be other factors contributing to drop in velocity head but not necessarily attributable to Mannings' n. Nevertheless at manhole, Mh5 of n = 0.011 is for lined canal with neat cement surface. This description fitted the condition of channel under investigation for it had deposits but no growth or trash in it.

Table 4: Calibration and Validation of Manning's n
1Error is computed as the average difference Da, being a percent of the hydraulic depth

Profile and Flowrate (m3/s)	Average observed depth of flow (m)	Experimental Estimate of n-value			Calibrated n-value			Model Validation		
		n	Da (m)	Error1 %	n	Da (m)	Error %	n	Da (m)	Error %
PF2 0.507	0.81	0.013	0.53	65.2	0.032, 0.011, 0.011	0.18	2.06	-	-	-
PF3 0.499	0.81	0.013	0.58	71.3	0.032, 0.011, 0.011	0.20	6.58	-	-	-
PF4 0.445	0.70	0.013	0.57	81.8	0.032, 0.011, 0.011	0.1467	0.38	-	-	-
PF1 0.711	1.12	-	-	-	-	-	-	0.032, 0.011, 0.011	0.12	21.4
PF5 0.590	0.87	-	-	-	-	-	-	0.032, 0.011, 0.011	0.39	44.2

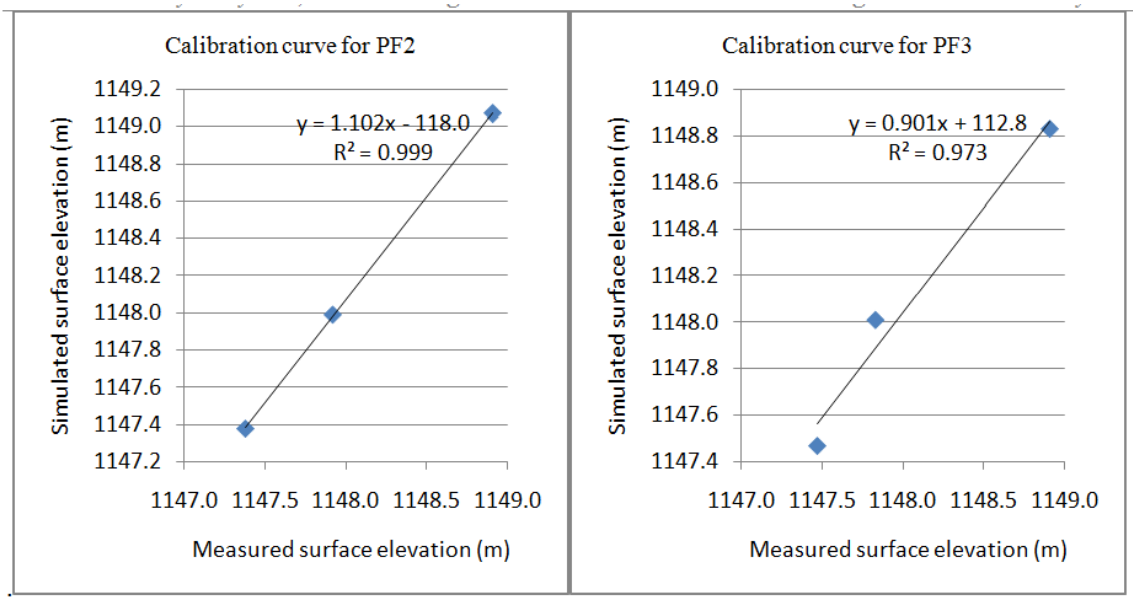

(a) Profile PF2

(b) Profile PF3

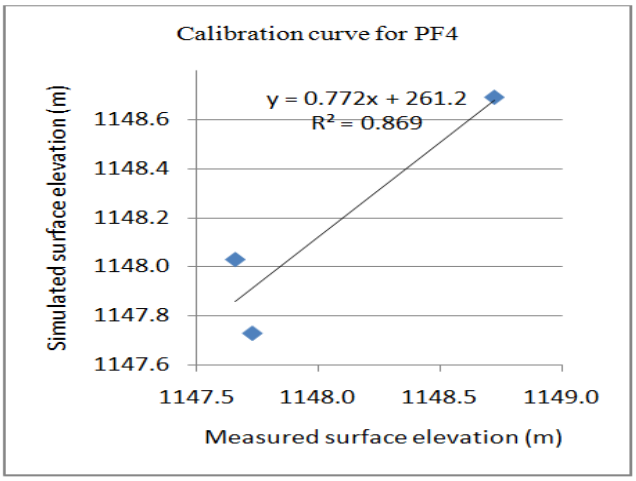

(c) Profile PF4

Figure 4: Calibration curves for profiles (a) PF2, (b) PF3 and (c) PF3

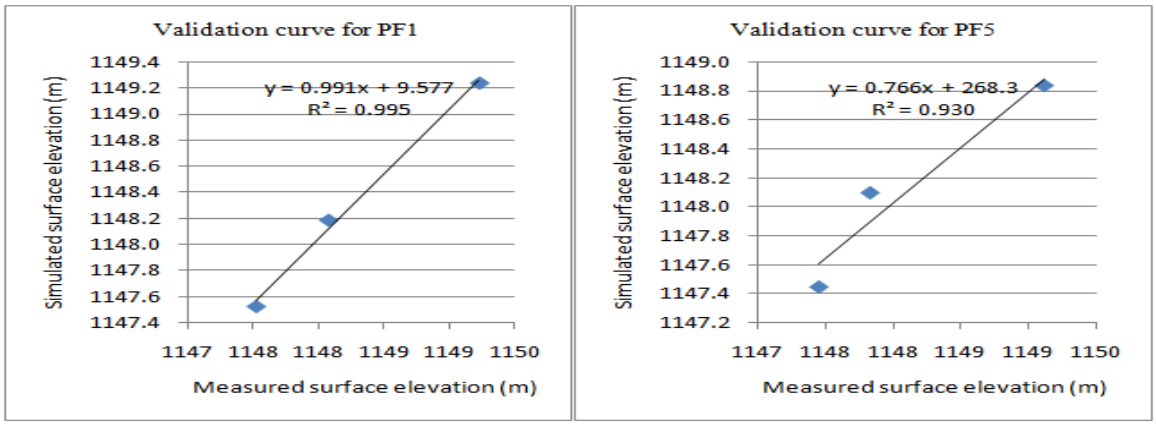

(a) Profile PF1 (b) Profile PF5

Fig. 5: Validation curves for profiles (a) PF1, (b) PF5

In all cases the simulated water surface level for manhole station 245(Mh3), was above the observed values as indicated in TABLE 4 and Fig.6, 7, 8, 9 and 10suggesting that there is a likelihood of pooled water at that section under normal circumstances of open channel flow. The low value of measured water level could be due to restriction of free surface flow by the canal walls.

Table 5: Calibration and validation results for water surface levels

Model Run	Profile	Discharge (m3/s)	Station */ Manhole	Measured water level		Simulated water level n=0.011				
				Measured Surface Elevation (m)	Invert Level (m)	Simulated Surface Elevation (m)	a	b	R^2	w R^2
Calibration	PF2	0.507	602/Mh1	1148.91	1148.07	1148.91	-118.5	1.10	1.00	0.91
			245/Mh3	1147.92	1147.06	1148.33				
			0/Mh5	1147.38	1146.64	1147.38				
	PF3	0.499	602/Mh1	1148.91	1148.11	1148.90	112.88	0.90	0.97	0.87
			245/Mh3	1147.83	1147.05	1148.32				
			0/Mh5	1147.47	1146.75	1147.47				
	PF4	0.445	602/Mh1	1148.72	1148.14	1148.80	261.23	0.77	0.87	0.67
			245/Mh3	1147.66	1147.05	1148.29				
			0/Mh5	1147.73	1146.83	1147.73				
Validation	PF1	0.711	602/Mh1	1149.23	1147.88	1149.15	9.58	0.99	1.00	0.99
			245/Mh3	1148.08	1147.02	1148.48				
			0/Mh5	1147.53	1146.57	1147.53				
	PF5	0.590	602/Mh1	1149.12	1148.15	1149.03	268.34	0.77	0.93	0.72
			245/Mh3	1147.83	1147.02	1148.39				
			0/Mh5	1147.45	1146.62	1147.45				

*The station name is represented by the distance along the canal axis, in meters, between it and the farthest downstream station.

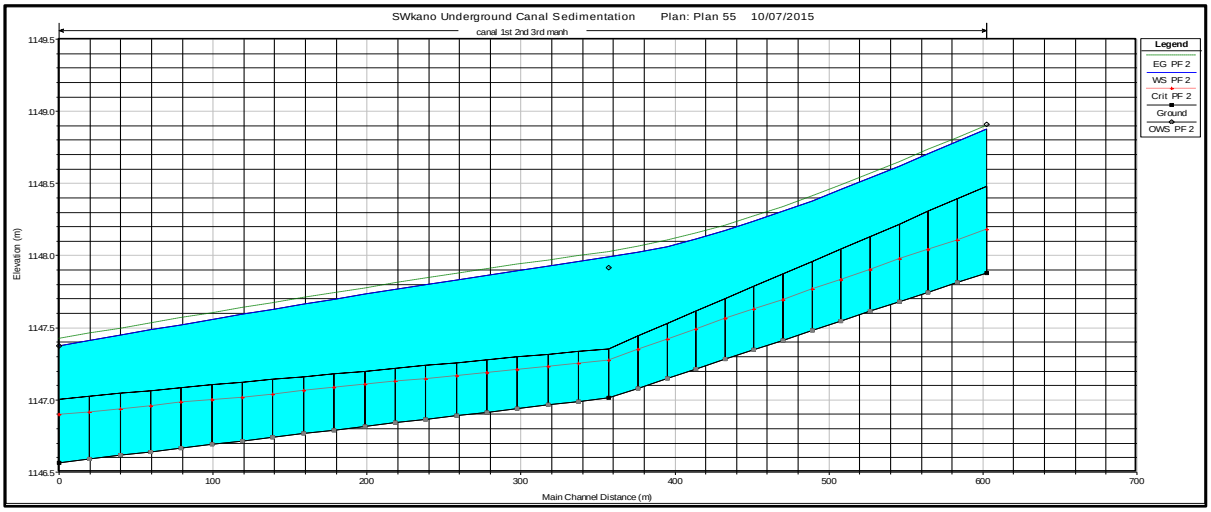

Figure 6: HEC-RAS calibration profile output for profile PF2

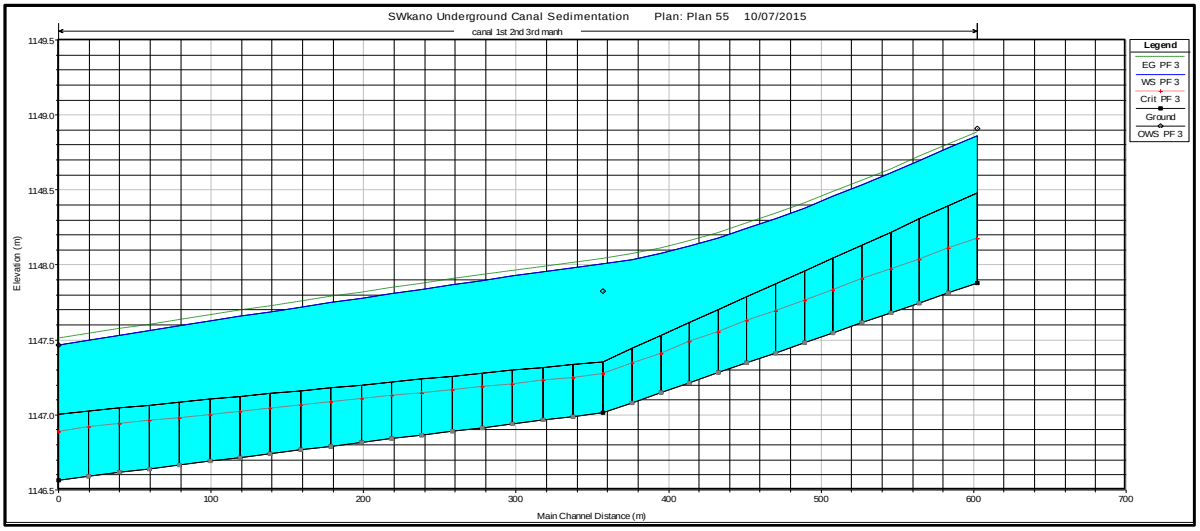

Figure 7: HEC-RAS calibration profile output for profile PF3

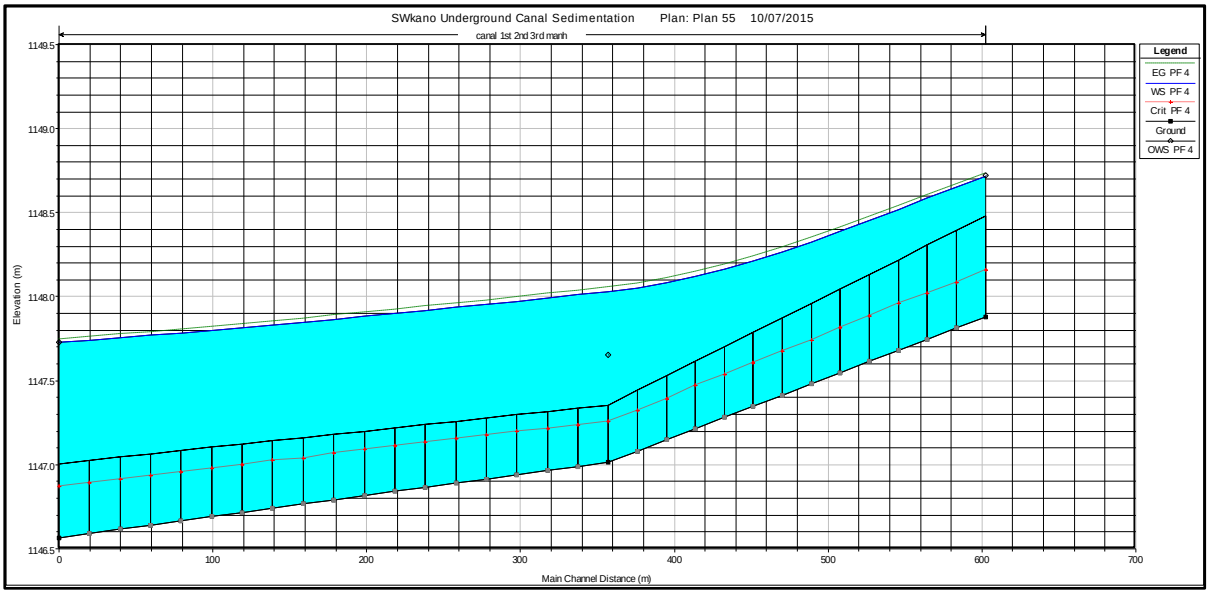

Figure 8: HEC-RAS calibration profile output for profile PF4

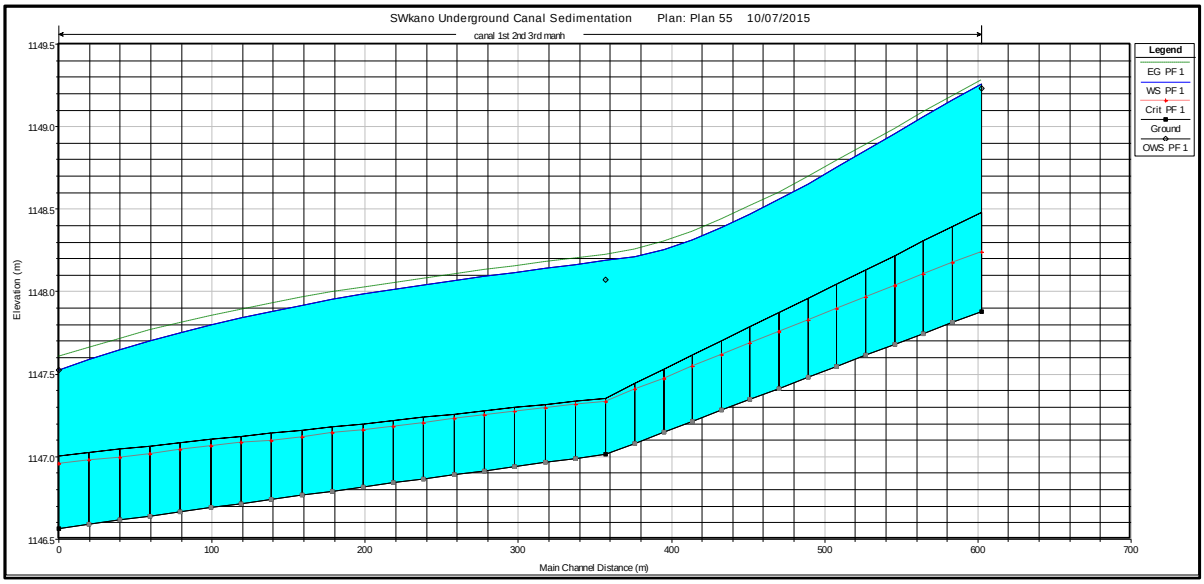

Figure 9: HEC-RAS validation profile output for profile PF1

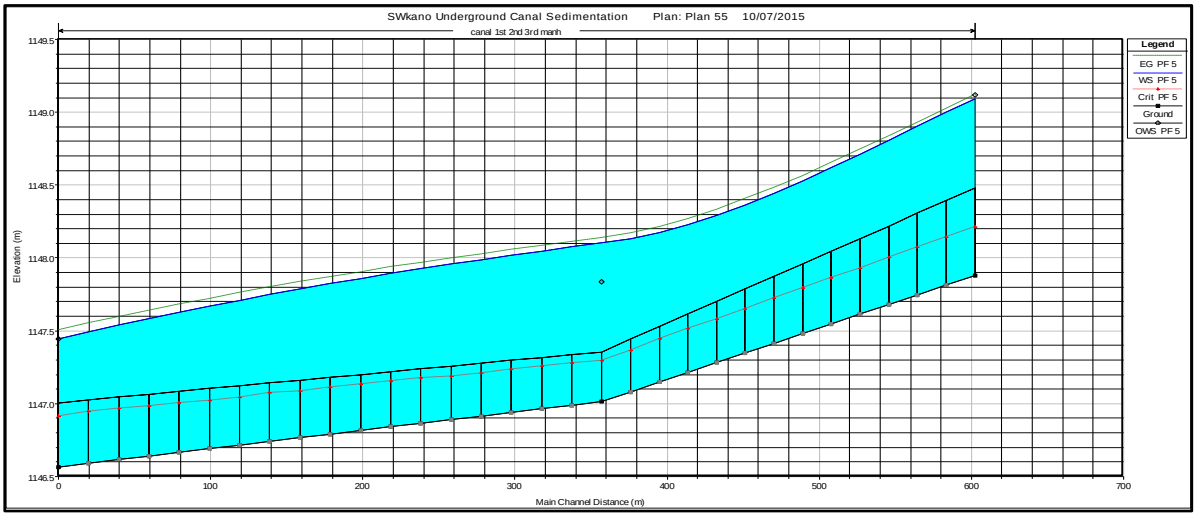

Figure 10: HEC-RAS validation profile output for profile PF5

The second phase of HEC-RAS model calibration for sediment transport was done after running the steady flow simulation. The calibration of sediment entrainment parameters, coefficients and exponents in HEC-RAS were eventually done through parameter optimisation. The eventual best fit curve of simulated against observed sediment discharge was based on the assumption that the flow entering the canal was at equilibrium sediment load. The first manhole (Mh1) hydraulic data was used for calibration. All manholes were assumed to have similar canal bed sediment characteristics for each simulation. The third manhole (Mh3) and fifth manhole (Mh5) hydraulic data were used for validation. The model input parameters for calibration were determined through physical measurement, computation or generated from inbuilt algorithms of HEC-RAS model. The initial conceptual parameter values used for simulation were determined from sediment particle, d50, size below which 50% of the particles would be transported. The value of d50 was determined from laboratory measurements as 0.65 mm. Those initial parameters were: critical mobility parameter A=0.17, coefficient, C=0.025 and exponent, m=1.78. The critical mobility parameter was the most sensitive parameter in Ackers and White sediment transport equation.

The eventual calibrated values, after optimisation, were A=0.20, C=0.004 and m=4. However, there were other conceptual parameters which were not exposed to calibration by the model thus; exponent n and constant α. The value of α was taken to be equivalent to 10 as provided for in the model and the exponent, n, being a function of sediment properties, never needed calibration. Tabulated in TABLE5 and graphically represented in Fig.11, Fig.12, Fig.13 and Fig.14 are the simulated and measured sediment discharge values at each manhole during experimental, calibration and validation processes.

Table 5: Calibration and validation results for cumulative sediment discharge

Model run type and properties	Date	Time	Discharge (m^3/s)	Simulated (ton)	Measured (ton)	Description of line of best fit			
						a	B		wR^2
Experimental Manhole 1 (Mh1) A=0.195, C=0.031, m=2.06	15/9/2011	11.28am	0.711	1.17	158.09	1.3694	-196.00		0.3672
	16/9/2011	09.23am	0.507	74.92	167.84				
	16/9/2011	12.45pm	0.499	87.72	703.58				
	26/9/2011	11.09am	0.445	1116.04	705.68				
	26/9/2011	01.47pm	0.590	1126.88	737.97				
Calibration Manhole 1 (Mh1) A=0.2, C=0.004, m=4	15/9/2011	11.28am	0.711	1.72	158.09	1.3027	-174.21		0.3922
	16/9/2011	09.23am	0.507	94.99	167.84				
	16/9/2011	12.45pm	0.499	106.82	703.58				
	26/9/2011	11.09am	0.445	1068.19	705.68				
	26/9/2011	01.47pm	0.590	1078.95	737.97				
Validation Manhole 3 (Mh3) A=0.2, C=0.004, m=4	15/9/2011	11.28am	0.711	3.24	296.59	0.2899	21.113		0.1454
	16/9/2011	09.23am	0.507	219.29	306.61				
	16/9/2011	12.45pm	0.499	182.52	871.39				
	26/9/2011	11.09am	0.445	322.57	873.85				
	26/9/2011	01.47pm	0.590	326.13	922.87				
Validation Manhole 5 (Mh5) A=0.2, C=0.004, m=4	15/9/2011	11.28am	0.711	8.93	283.19	0.8628	-116.63		0.5342
	16/9/2011	09.23am	0.507	272.67	294.80				
	16/9/2011	12.45pm	0.499	277.77	768.59				
	26/9/2011	11.09am	0.445	693.58	775.44				
	26/9/2011	01.47pm	0.590	699.06	816.39				

The initial estimated values of the conceptual parameters used to draw the experimental curve in Fig.11 display a coefficient of correlation, R2, of 0.5029. This corresponding weighted value, wR2, was 0.3672, an indication that there was over-prediction of sediment discharge of 36.94%. The calibration curve in Fig.12 was arrived at after further optimisation simulation runs giving values of R2 and wR2 of 0.5109 and 0.3922 respectively. In this case over-prediction dropped to 30.27%. The over-prediction characteristic of Ackers and White sediment transport equation was confirmed by Hassanzadeh et.al.,(2011) where it was concluded that the equation overestimated total sediment load. The calibration simulated results showed a drop in the error factor from 63.28% to 60.78%. The weighted correlation error was within the error factor of ± 100% documented as the finding from application of "more reliable methods" of sediment transport prediction. (Depeweg and Mendez, 2002).

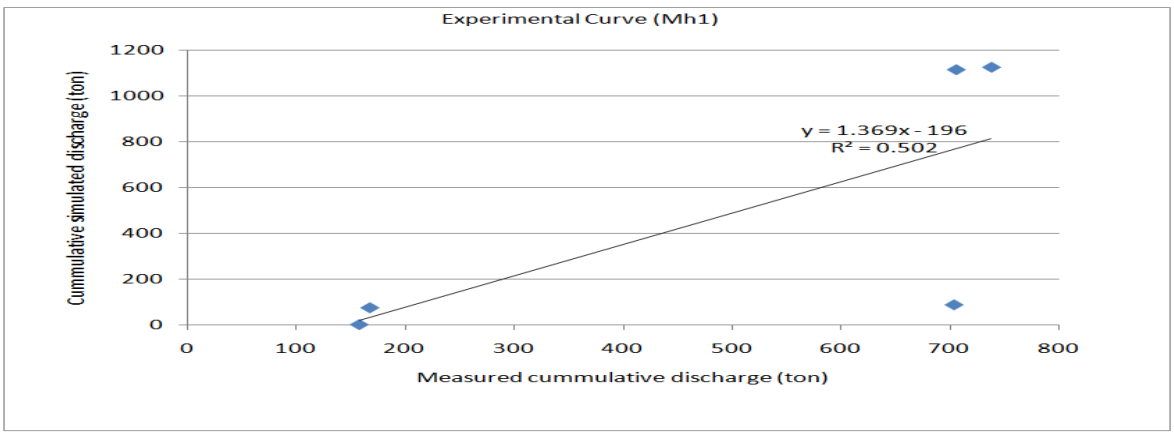

Figure 11: Initial experimental cumulative sediment discharge curve (Mh1)

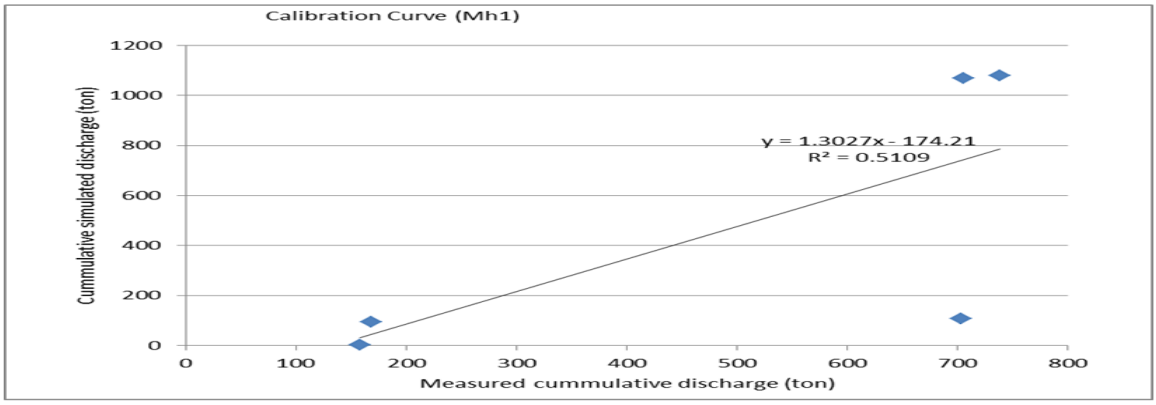

Figure 12: Calibration cumulative sediment discharge curve (Mh1)

The validation of the model as shown in Fig.13 and Fig.14, indicated that the discharge for manhole 3 (Mh3) and manhole 5 (Mh5) had correlation errors of 49.85% and 38.09% respectively. However their respective weighted correlation coefficient wR2 stood at 0.1454 and 0.5342, signifying that there was more under-prediction in manhole 3 (Mh3) than Manhole 5 (Mh5) as shown in the validation graph in Fig.13 and Fig.14. The under-prediction phenomenon was due to formation of armoured sediment layer on the canal bed for continuous flow. The armoured layer was, in practice, interfered with by periodical temporary canal closure for maintenance. Previously suspended particles could have settled on the bed thereby interfering with the assumed armoured layer. The settled particles increased the quantity of sediment available for transport.

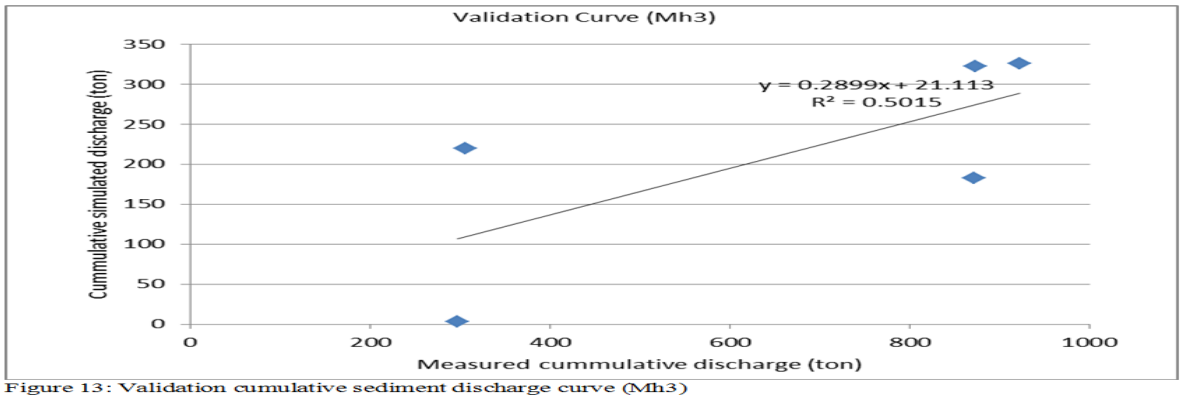

Figure 13: Validation cumulative sediment discharge curve (Mh3)

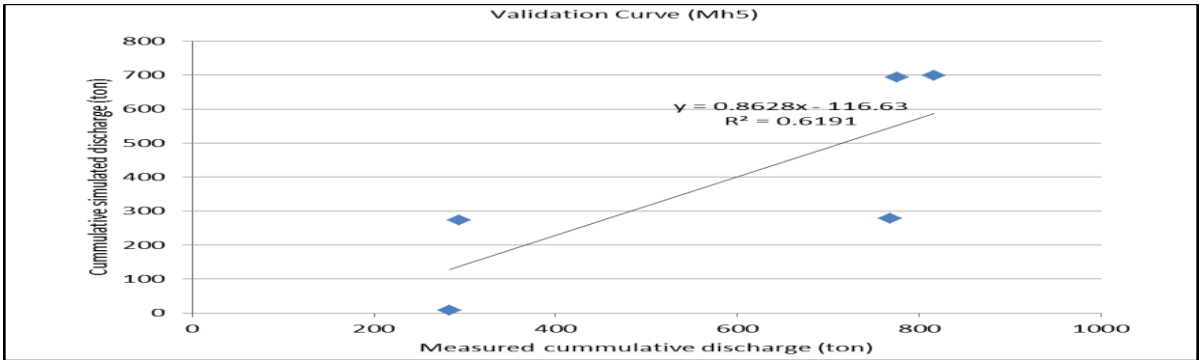

Figure 14: Validation cumulative sediment discharge curve (Mh5)

a. Simulation of HEC-RAS Model for 0.25, 0.50, 0.75 and full flow scenarios.

The simulation was done for the selected scenarios for the purposes of plotting sediment rating curve from which other flow scenarios could be predicted. The conceptual parameters remained as calibrated except the value on Manning's roughness coefficient which was set at finished concrete surface, with gravel on bottom, n=0.017 (Chow 1959). The Manning's coefficients obtained earlier were not used due to an assumed concrete surface without deposits. The discharge and respective water surface elevations, as derived from equations 20, 21 and 22 and tabulated in TABLE 6, were used for simulation.

Table 6: Discharge values for different flow scenarios

Flow scenario	Depth D (m)	Water Surface Elevation (m)	Slope S	Hydraulic radius R (m)	Velocity v (m/s)	Angle Ø (radians)	Cross section area (m2)	Flow scenario Discharge Q (m3/s)
0.25	0.375	1146.63	0.002447	0.2199	1.06	2.09	0.35	0.366
0.50	0.75	1147.01	0.002447	0.375	1.51	3.14	0.883	1.337
0.75	1.125	1147.38	0.002447	0.4525	1.72	4.19	1.42	2.438
1.00	1.5	1147.76	0.002447	0.375	1.51	6.28	1.77	2.674

The HEC-RAS model was run with sets of input data for the specified scenarios to give respective outputs of cumulative sediment discharge at a time step of 30 days. The boundary condition for sediment load series was set at 0.5 kg/s, being the average load over the observation period. Observed storm load of 2.0 kg/s was excluded from this average since simulation results indicated that the canal got blocked before the expiry of simulation time step of 30 days. The discharge for each scenario is shown in TABLE 7 below.

Table 7: Cumulative sediment discharge for different discharge scenarios

Flow scenario water discharge		Total cumulative sediment discharge at intake		Total cumulative sediment discharge at outlet	
m3/s	Log(m3/s)	kg/s	Log(kg/s)	kg/s	Log(kg/s)
0.366	-0.43652	18.46535	1.266357	11.4931	1.060437
1.337	0.126131	87.25224	1.940777	85.57523	1.932348
2.438	0.387034	198.9619	2.29877	191.6585	2.282528
2.764	0.441538	216.4992	2.335456	208.5372	2.319184

The model assumed state of equilibrium sediment transport capacity at intake and therefore the boundary condition load was much lower than the sediment discharge at outlet in all flow scenarios. Water discharge increased linearly with the cumulative sediment discharge plotted on a logarithmic scale at both canal intake and outlet as shown in Fig. 15. Inlet and outlet sediment curves converge with increase in discharge meaning that higher percentage of sediment entering the canal got transported to the outlet without deposition with increase in discharge.

Ideally, for no deposition, inlet sediment load should be equal to the sediment discharge at underground canal outlet. However this may not be the case since the bed gradient is not uniform in the canal. There may appear that the sediment entering the canal is equivalent to sediment outflow and still the canal would get blocked due to temporal deposition and entrainment taking place at different points along the canal. Simulation of sediment transport capacity for each class (see TABLE8) was necessary to evaluate which particles were predominantly discharged at each manhole.

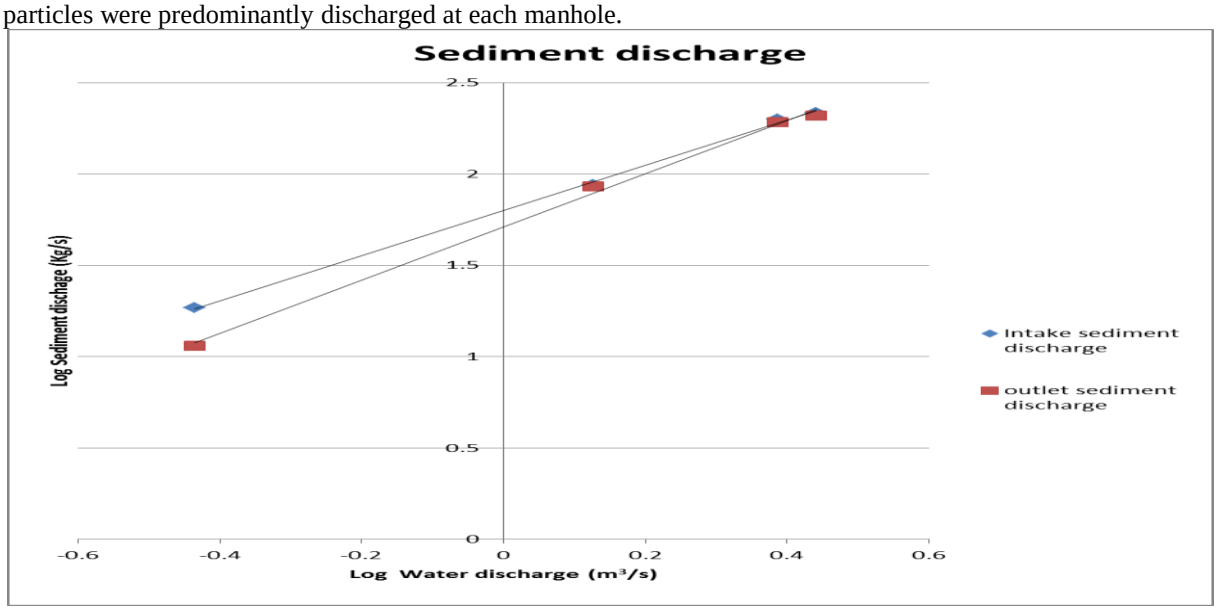

Figure 15: Simulated sediment discharge at intake and outlet.

Each flow scenario was simulated for a time step of 30 days to determine sediment transport capacity at each manhole so as to evaluate whether all classes of sediment particles entering an observation station are transported through. The classes ranged from class 5 to 11 as in TABLE8 adopted from grain size classification by American Geophysical Union. These were the grain classes sampled from canal bed at each manhole. The simulation results for the lowest discharge scenario, of 0.366 m/s are shown in Fig. 16, Fig. 17 and Fig. 18.

Table 8: Grain size classification

Grain Class	Description	Grain diameter range (mm)
5	Coarse silt	0.032-0.0625
6	Very fine sand	0.0625-0.125
7	Fine sand	0.125-0.250
8	Medium sand	0.250-0.5
9	Coarse sand	0.5-1.0
10	Very coarse sand	1-2
11	Very fine gravel	2-4

SOURCE: U.S. Army Corps of Engineers (2002).

Simulated total transport capacity increased with discharge at each manhole. Manhole 5 (Mh5) had the highest transport capacity followed by manhole 1 (Mh1) and manhole 3 (Mh3) in that order for different flow scenario water discharge values: 1.337 m3/s, 2.438 m3/s and 2.674 m3/s. Transport capacity depended on flow velocity and Mh5, having the highest bedslope, exhibited the highest transport capacity. Change of bedslope at Mh3 drastically reduced its transport capacity. At Mh1 the flow velocity was higher than at Mh3 due to uniform bedslope and lack of pooled water at the section. This showed that there is net deposition at Manhole 3 while further entrainment of previously deposited particles occurred at Manhole 5, which was also dependent upon the supply of sediment available from upstream sources. The entrainment phenomena may be misleading since sediment transport is limited by sediment availability. This case is termed supply-limited (Julien, 1998). At flow scenario of 0.366 m3/s transport capacity decreased gradually from manhole 1, through manhole 3 to manhole 5; implying there was net deposition at manhole 3 and manhole 5.

Transport capacity at manhole 1 (Mh1) for all grain classes available was above zero for all flow scenarios except for grain classes 10 and 11 whose capacity was comparatively low. At manhole 3 (Mh3) transport capacity was zero for both grain classes 10 and 11 for all flow scenarios. This shows that previously transported grain classes 10 and 11 via manhole 1 would be deposited at manhole 3. Canal section at Manhole 3 is most likely to get blocked from piling deposits of grains 10 and 11 for all flow scenarios. Flow scenario discharge, 0.366 m3/s, recorded zero transport capacity at manhole 5 (Mh5) for grain classes 8, 9 and 11. Manhole 5 is likely to block only during low flows due to piled deposits of grain classes 8, 9 and 10. Change in bed slope may eventually give rise to deposits piling at Manhole 1 as well.

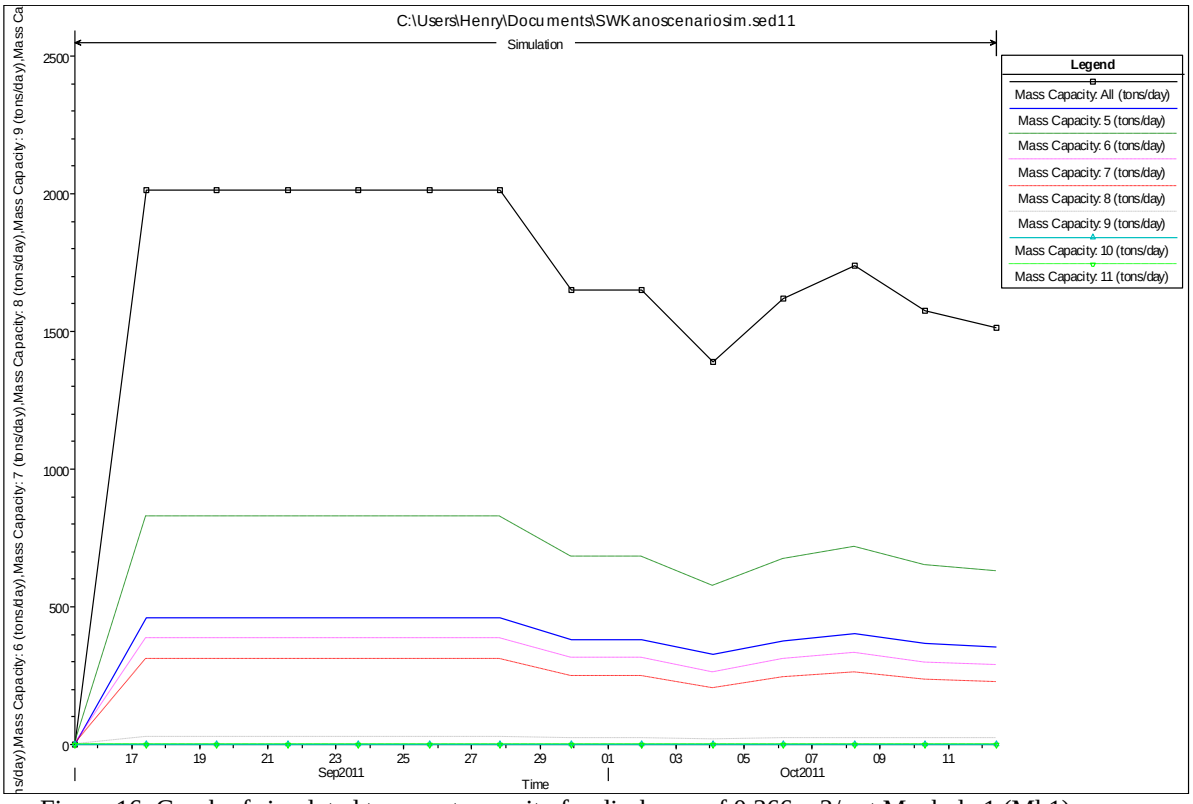

Figure 16: Graph of simulated transport capacity for discharge of 0.366 m3/s at Manhole 1 (Mh1)

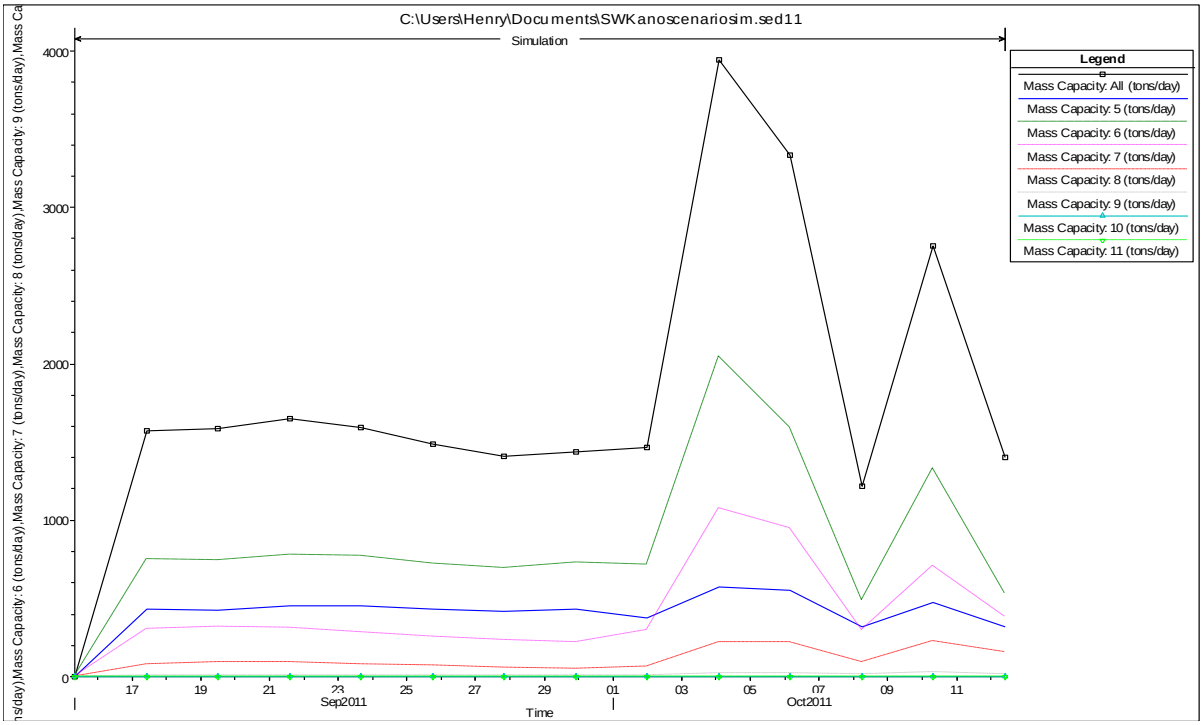

Figure 17: Graph of simulated transport capacity for discharge of 0.366 m3/s at Manhole 3 (Mh3)

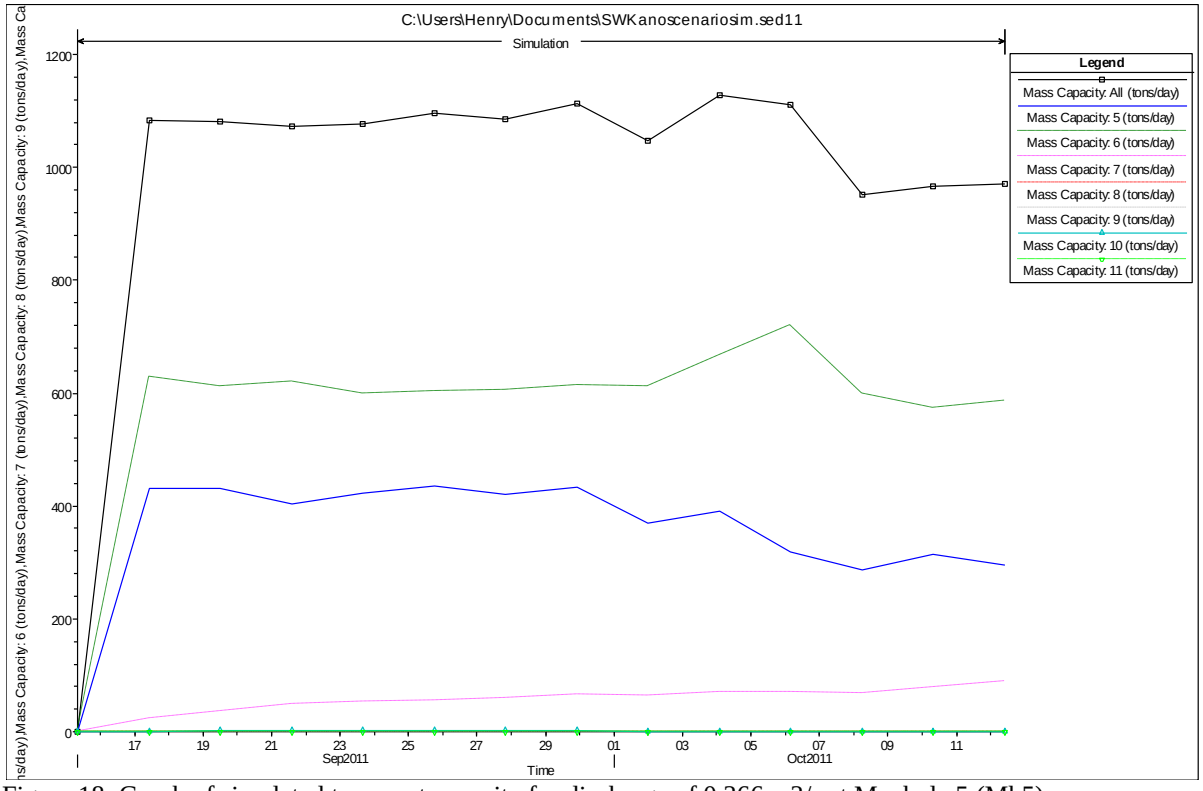

Figure 18: Graph of simulated transport capacity for discharge of 0.366 m3/s at Manhole 5 (Mh5)

IV. CONCLUSION AND RECOMMENDATION

During calibration of the HEC-RAS model, the manning's roughness coefficient between manhole 1 and manhole 3 was 0.032 and that of manhole 3 and manhole 5 was 0.011. This was because the reduced slope induced much finer grains to settle at the bed hence reducing the value of Manning's roughness coefficient downstream. The conceptual parameters were calibrated as A=0.20, C=0.004 and m=4. These calibration values could be used to predict sediment transport within the canal since the deviation of predicted and measured values were within the acceptable range of ± 100%. For better prediction more sets of data need to be observed to increase the accuracy of calibrated values.

HEC-RAS model simulation indicated a selective grain size sediment transport. This would vary from one observation point to the other and would vary with canal discharge. The sediment load that can be carried through the canal without deposition would therefore not depend entirely on sediment concentration but also on grain size percent composition and the prevailing bed slope. The grain sizes 8, 9, 10 and 11 should be screened from entering the canal to avoid sediment deposition within the canal. With increase in flow discharge a higher proportion of sediment entering the canal would be discharged at the outlet. Higher flow discharge is necessary in order to minimise deposition.

Irrigation canals conveying water with high sediment load should not be operated during flood flows as the bed slope of the river is usually higher than the irrigation canal bed slope meaning equilibrium sediment transport in the river becomes source of sediment deposits as soon as it enters the canal. This problem is aggravated by reduction of slope further downstream of irrigation canal. Piped flows are more likely to block at the point where the bed slope changes to become gentler.

REFERENCES

[1] Ayibotele, N. B. and Tuffour-Darko , T. (1979). Sediment Loads in the Southern Rivers of Ghana. Accra, Ghana: Water Resources Research Unit.

[2] Chow, V.T. (1959). Open-channel hydraulics. New York, McGraw-Hill.

[3] Depeweg, H. and Mendez, N. V. (2002). Sediment transport applications in irrigation canals. Wiley InterScience Journal, Irrigation and Drainage, 51, 167–179.

[4] Depeweg, H. and Mendez, N. V. (2006). A new approach to sediment Transport in the design and operation of Irrigation Canals. USA: Routledge.

[5] Finkner, F. C., Nearing, M. A., Foster, G. R., Gilley, J. E. (1989) A Simplified Equation for Modelling Sediment Transport Capacity. Journal of ASAE 32(5), 1545-1550.

[6] Hassanzadeh, H., Faiznia, S., Bajestan, M., and Motamed, A. (2011). Estimate of SedimentTransport Rate at Karkheh River in Iran Using Selected Transport Formulas. Journal of World Applied Sciences Journal 13(2), 376-384.

[7] Hoel, P. G. (1984). Introduction to mathematical statistics. Canada: John Wiley and Sons.

[8] McCully, P. (1996). The Ecology and Politics of Large Dams. London: Zed Books.

[9] Onyando, J. O., Kisoyan, P. and Chemelil, M. C. (2004). Estimation of potential soil erosion of river Perkerra catchment in Kenya. Journal of Water Resources Management, 19, 133–143.

[10] Parhi, P. K., Sankhua, R. N., Roy G. P. (2012). Calibration of Channel Roughness for Mahanadi River, (India) Using HEC-RAS Model, Journal of Water Resource and Protection, 4, 847-850.

[11] Santhi, C., Arnold, J. G., Williams, J. R., Dugas, W. A., Srinivasan, R. and Hauck, L. M. (2001) Validation of the SWAT model on a large river basin with point and nonpoint sources. Journal of American Water Resources Assoc. 37(5), 1169-1188.

[12] Spillios, L. C. (1999). Sediment intrusion and deposition near road crossings. Unpublished master's thesis, University of Alberta, Alberta, Canada.

[13] ASCE(1975). Sedimentation Engineering. American Society of Civil Engineering Manual No. 54, V. A. Vanoni, editor.

[14] Huang, J.V. and Bountry, J. (2009) DRAFT SRH-Capacity User Manual Version 1.37, U.S.Dept. of the Interior, Bureau of Reclamation, Technical Service Center, Denver CO.

[15] Ackers, P. and White, W. R. (1973). Sediment transport: new approach and analysis. ASCE Journal of Hydraulic Division, 99(11), 2041-2060.

[16] U.S. Army Corps of Engineers (2002). HEC-RAS Hydraulic Reference Manual, Version 3.1, November 2002, CPD-69. Davis, CA: The Hydraulic Engineering Centre.

[17] Xiaoqing, Y. (2003). Manual on sediment Management and Measurement. Operational Hydrology Report, 47.